Soft Matter

Accepted Manuscript

This is an *Accepted Manuscript*, which has been through the Royal Society of Chemistry peer review process and has been accepted for publication.

Accepted Manuscripts are published online shortly after acceptance, before technical editing, formatting and proof reading. Using this free service, authors can make their results available to the community, in citable form, before we publish the edited article. We will replace this *Accepted Manuscript* with the edited and formatted *Advance Article* as soon as it is available.

You can find more information about *Accepted Manuscripts* in the Information for Authors.

Please note that technical editing may introduce minor changes to the text and/or graphics, which may alter content. The journal's standard Terms & Conditions and the Ethical guidelines still apply. In no event shall the Royal Society of Chemistry be held responsible for any errors or omissions in this *Accepted Manuscript* or any consequences arising from the use of any information it contains.

ROYAL SOCIETY OF CHEMISTRY

www.rsc.org/softmatter

Cite this: DOI: 10.1039/c0xx00000x

www.rsc.org/xxxxxx

ARTICLE TYPE

Calorimetric evidence for a mobile surface layer in ultrathin polymeric films: Poly(2-vinyl Pyridine)

Sherif Madkour[a], Huajie Yin[a], Marieke Füllbrandt[a,b], Andreas Schönhals[a]**

Received (in XXX, XXX) Xth XXXXXXXXX 20XX, Accepted Xth XXXXXXXXX 20XX

DOI: 10.1039/b000000x

Specific heat spectroscopy was used to study the dynamic glass transition of ultrathin poly(2-vinyl pyridine) films (thicknesses: 405 - 10 nm). The amplitude and the phase angle of the differential voltage were obtained as a measure of the complex heat capacity. In a traditional data analysis, the dynamic glass transition temperature T_g is estimated from the phase angle. These data showed no thickness dependency on T_g down to 22 nm (error of the measurement of ± 3 K). A derivative-based method was established, evidencing a decrease in T_g with decreasing thickness up to 7 K, which can be explained by a surface layer. For ultrathin films, data showed broadening at the lower temperature side of the spectra, supporting the existence of a surface layer. Finally, temperature dependence of the heat capacity in the glassy and liquid states changes with film thickness, which can be considered as a confinement effect.

1. Introduction

The characterization of the glass transition temperature, T_g, of ultrathin polymer films has been of great interest due to their numerous applications in fields like coatings, membranes, and innovative organic electronics. Scientifically, ultrathin films provide ideal sample geometry for studying the confinement effects on the glass transition of polymers; as film thicknesses can be easily tuned by spin coating [1]. Generally, glass transition is a topical problem of soft matter research (see for instance [2-7]). Investigations on highly confined systems may help to evidence the existing of a dynamical length scale [8] corresponding to the glass transition, which is difficult to measure by other approaches.

Since the pioneering work of Keddie et al. [9,10], the thickness dependence of the glass transition temperature has been controversially discussed in the literature. For the same polymer/substrate systems, divergent results have been published. In a recent perspective discussion by Ediger et al. [11], the progress made in the last years was discussed (see for instance [12-20]). For polymers supported by a non-attractive substrate (see for instance [10,15,21-27]) a depression of the thermal glass transition temperature T_g with decreasing film thickness is widely observed. This T_g depression is discussed to originate as a result of a free polymer/air surface having a higher molecular mobility than the bulk due to missing polymer-polymer segment interactions and also due to structural differences [11,15]. Recently, optical photobleaching experiments [14, 28], as well as the embedding of gold nanospheres into a polymer surface [29,30], provided some evidence for a highly mobile surface layer.

For polymers having a strong interaction with the substrate, T_g may increase with the reduction of the film thickness [31-33]. These experimental results were explained by the formation of an adsorbed boundary layer, in which the polymer segments have a lower molecular mobility; hence a higher glass transition temperature [34]. For that reason, attempts are made to correlate depression or increase of the glass transition temperature with the interaction energy between the surface of the substrate and the polymer γ_{SP} [35]. A depression of T_g should be observed for values of γ_{SP} smaller than a critical value γ_c, because the influence of the mobile surface layer should be dominant in this case. For $\gamma_{SP}>\gamma_c$ the reduced mobility layer at the substrate will dominate and an increase of T_g should be expected. This concept was critically considered by Tsui et al. [36], with the conclusion that the interaction energy between the polymer segments and the surface of the substrate is not the only relevant parameter. Also the packing of the segments at the interface might play a role. In general, no correlation between γ_{SP} and the change of T_g with the film thickness was found [7]. Nowadays, there is growing consensus that the T_g shifts observed in ultrathin films compared to the bulk are related to the combined influence of the free surface (polymer-air) and the polymer-substrate interfacial interaction [11]. Even though the free surface is assumed to speed up the segmental dynamics, at temperatures near T_g, the effect of the polymer-substrate interaction can either increase or decrease the dynamics, and consequently the relaxation times of the adjacent polymer segments.

Generally, there are two different experimental approaches to investigate the glass transition of ultrathin polymer films. In the first approach (also called static experiments), the temperature is ramped and a thermodynamic property (or an associated quantity) is measured. A change in the temperature dependence of this quantity is interpreted as thermal glass transition, where a corresponding thermal glass transition temperature (T_g) can be extracted. Examples for these methods are ellipsometry [10,15], DSC [43] or Flash DSC [26], fluorescence spectroscopy [37], dielectric expansion dilatometry [22,23,32], or X-ray reflectivity [38], just to mention a few. In the second approach, techniques that directly explore the segmental mobility, like dielectric (see for instance [19,32,33]) or specific heat spectroscopy [19,39-42] have

Soft Matter Accepted Manuscript

been employed. In these cases, a dynamic glass transition temperature is measured which is higher than the thermal one. So far, all investigations carried out by specific heat spectroscopy did not show a thickness dependence of the dynamic glass transition temperature, even in cases where simultaneous dilatometric experiments evidenced a decrease of the thermal glass transition temperature [43]. A possible reason for that is discussed in reference [11]. Moreover by employing cooling rate dependent experiments like ellipsometric [23,25], photobleaching [14] or Flash DSC [26] experiments it was evidenced that there is a limiting cooling for the depression of the thermal T_g. For instance, for polystyrene the value of this limiting cooling rate was found to be higher than 90 K/min [25].

This study focuses on the investigation of the dynamic glass transition of thin films of poly(2-vinyl pyridine) (P2VP), as contradicting results exist in the literature. In an X-ray reflectivity study of P2VP films on acid cleaned SiO_2 surface, the thermal glass transition temperature T_g increases with decreasing film thickness up to 20 – 50 K compared to the bulk value [38]. These results are also consistent with more recent data [44,45] and were explained assuming strong interactions of the polymer segments with surface of the substrates. Moreover, a similar behavior was observed for thin P2VP films capped between aluminum layers in a dielectric study [46]. Moll and Kumar found only a small shift in T_g for P2VP/ silica nanocomposites [47]. Holt et al. [48] report also a study on P2VP filled with silica nanoparticles. An adsorbed boundary layer around the nanoparticles with a thickness of ca. 4 nm was found having a two-order of magnitude reduced mobility compared to the bulk P2VP, hence a higher glass transition temperature consistent with findings discussed above. A similar result was reported for poly(vinyl acetate) filled with silica nanoparticles [49]. These results are in contradiction to an investigation of P2VP films spin coated on a highly doped Si wafer by broadband dielectric spectroscopy [50] where the dynamic glass transition was found to be independent of the film thickness. Also semi-isolated P2VP chains adsorbed on a doped Si wafer seem to resemble bulk like dynamics [20]. These results are also consistent with data obtained by high speed chip calorimetry where also a thickness independent T_g value for ultrathin P2VP films was found [51]. Paeng et al. employed photobleaching techniques to explore the dynamics of thin P2VP films on the cleaned native surface of a SiO_2 wafer [52]. A highly mobile surface layer at the polymer/air interface was evidenced. However, indications for a reduced mobility layer at the surface of the substrate were also reported.

Here specific heat spectroscopy is employed utilizing AC-chip calorimetry [39] to investigate the dynamic glass transition of thin P2VP films. These measurements are accompanied by contact angle measurements in order to quantify the interaction of the P2VP segment with a SiO_2 surface used as substrate. Additionally, broadband dielectric spectroscopy is used to measure the molecular dynamics of the bulk material for comparison.

2. Experimental section

2.1. Methods

Specific heat spectroscopy: Specific heat spectroscopy is employed using differential AC-chip calorimetry [39]. The calorimetric chip XEN 39390 (Xensor Integration, NI) was used as measuring cell. The heater is located in the center of a freestanding thin silicon nitride membrane (thickness 1 µm) supported by a Si-frame with a window. This nanocalorimeter chip has a theoretical heated hot spot area of about 30 x 30 μm^2, with an integrated 6-couple thermopiles and two-four-wire heaters (bias and guard heater), as shown in reference [53]. Please note that in addition to the 30 x 30 μm^2 hot spot, the heater strips also contribute to the heated area. A SiO_2 layer with a thickness of 0.5 - 1 µm protects the heaters and thermopiles. The thin films are spin coated over the whole chip area, but only the small heated area was sensed and considered as a point heat source. Pictures of the sensor can be found in reference [41].

In principle the chip itself will contribute to the measured heat capacity. In the differential approach to AC-chip calorimetry, the contribution of the heat capacity of the empty sensor (without a sample) to the measured signal is minimized. In the approximation of thin films (submicron), the heat capacity of the sample C_S is then given by [39,40]

$$C_S = \frac{i\omega \bar{C}^2 (\Delta U - \Delta U_0)}{S P_0} \quad (1)$$

where ω is the angular frequency and i=$(-1)^{1/2}$ the imaginary unit. $\overline{C} \equiv C_0 + G/i\omega$ describes the effective heat capacity of the empty sensor (C_0 – heat capacity of the sensor; G/iω is the heat loss through the surrounding atmosphere), S is the sensitivity of the thermopile, P_0 is the applied heating power, and ΔU is the complex differential thermopile signal for an empty reference sensor and a chip with a sample, where ΔU_0 is the complex differential voltage measured for two empty sensors. A more detailed description of the calorimetric chip, its differential setup and the experimental method can be found in reference [39]. Absolute values of the heat capacity can be obtained by calibration procedures [40].

For the calorimetric measurement, the temperature scan mode was used. The temperature was scanned using a heating/cooling rate of 2.0 K/min at fixed frequency. After each heating/cooling run the frequency was changed stepwise in the range of 1 Hz - 10^4 Hz. The selected scanning rate and the used frequency range ensure stationary conditions for the measurement [54]. The heating power for the modulation was kept constant at about 25 µW, which ensures that the amplitude of the temperature modulation is less than 0.5 K [39] and so a linear regime. It is important to note that the measurements are carried out in the frame of the linear response theory. The estimated glass transition temperatures are dynamic glass transition temperatures and are taken in the equilibrium state. As discussed in detail in the introduction this is different form the temperature ramping experiments carried out in DSC [43], Flash DSC [26] or ellipsometric studies[23,25].

The PT-100 of the cryostat was calibrated by measuring phase transition temperatures for five different calibration substances, covering the whole temperature range of the calorimeter (173-573 K). The calibration equation obtained was then used to correct the collected temperature data [55].

Contact angle measurements: The measurements were carried out using the automated contact angle system G2 (Krüss) employing the static sessile drop method. The used test liquids were ethylene glycol, formamide, water and diiodomethane. Usually, 8 drops with a volume of 3 µl were dropped onto the surface of a thick

Soft Matter Accepted Manuscript

This journal is © The Royal Society of Chemistry [year]

sample film treated in a similar way as the thin layers. The mean contact angles were calculated from the average of at least 6 drops. The data for SiO_2 were taken from reference [41].

Broadband dielectric spectroscopy: For comparison, the dielectric properties of a bulk sample (50 µm) were measured by a high resolution Alpha analyzer with an active sample head (Novocontrol GmbH). The temperature was controlled by a Quatro cryosystem with a stability of 0.1 K. The sample for the dielectric measurements was obtained by melting P2VP between two gold plated brass electrodes (diameter 20 mm). Fused silica spacers controlled its thickness to be 50 µm.

2.2. Materials and sample preparation

P2VP was purchased from Polymer Standards Services GmbH (Germany) with a M_w of 1020 kg/mol and a PDI of 1.33. The thermal glass transition temperature is 373 K estimated by Differential Scanning Calorimetry (DSC, 10 K/min, second heating run). The selected polymer here is similar to the material used in reference [20] and allows therefore a direct comparison of the dielectric data. For the AC-chip calorimetry, the sensors were first mounted on the spincoater, a few drops of chloroform were added in the center, and then spin coated to rinse dust and organic contaminations. This procedure was repeated twice, followed by an annealing process of the empty chip at 473 K in vacuum for two hours to cure the epoxy resin completely, which is used to glue the chip to the housing.

P2VP was dissolved in chloroform with different weight percentages. The solutions were spincoated (3000 rpm, 60 s) onto the central part of the sensors. The film thickness was varied by adjusting the concentration of the solution. Note that all spin coating processes were carried out in a laminar flow box to minimize any possible contamination. Further, the films were annealed at 398 K ($T_{ann}=T_{g,Bulk}+25$ K) in an oil-free vacuum for 48 h, in order to remove the residual solvent and relax the stress induced by the spin coating procedure [56].

The thicknesses were measured for films identically prepared on silicon wafers with a native SiO_2 surface, because the film thicknesses cannot be directly measured at the sensor. Assuming that the surface of the silicon wafer has similar properties as the surface of the sensor, under identical spin coating and annealing conditions, corresponding film thicknesses will be obtained. To proof this assumption in more detail a XPS study is in preparation. The film thickness d was measured by the step height of a scratch across the film down to the wafer surface by an AFM Nanopics 2100 (see Fig. 1).

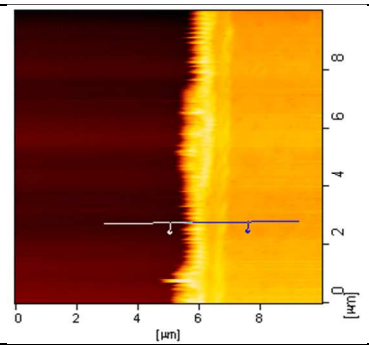

Fig. 1: AFM image of a scratch across a P2VP layer with a thickness of 50 nm on a silicon wafer.

Figure 2 gives the estimated film thicknesses versus the concentration of the solution. A linear dependence is observed, which goes to the point of origin as expected.

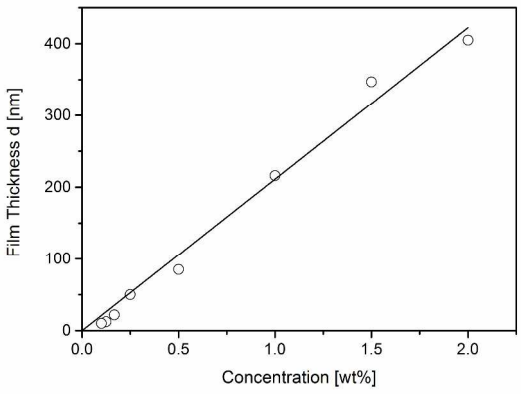

Fig. 2: Estimated film thickness d versus the concentration of the solution. The solid line is a linear regression to the data. The error bar is smaller than symbols used.

Moreover, the AFM topography image (Fig. 1) reveals no inhomogeneities and/or dewetting at the surface of the films. Also, a low surface roughness is observed. The root mean square (rms) roughness in the central area of the empty sensor was estimated to be about 3.5 nm [40]. The roughness of the film spin coated onto the surface of the sensor is lower and decreases with increasing film thickness. For a film thickness of ca. 10 nm, the roughness of the film on the sensor is comparable with that of a film prepared on a wafer [57].

3. Results and Discussion

The result of an AC calorimetry measurement yields a complex differential voltage as a function of frequency and temperature, which is proportional to the complex heat capacity (C^*_P) of the film. Here the real part of the complex differential voltage U_R and the phase angle ϕ are taken as measures of C^*_P. At the dynamic glass transition, U_R increases stepwise with increasing temperature (Fig. 3a) and ϕ shows a peak (Fig. 3b).

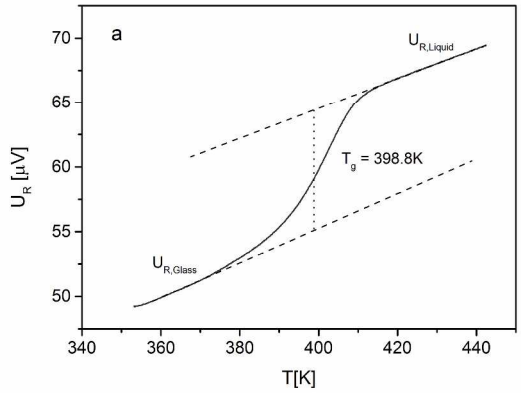

Soft Matter Accepted Manuscript

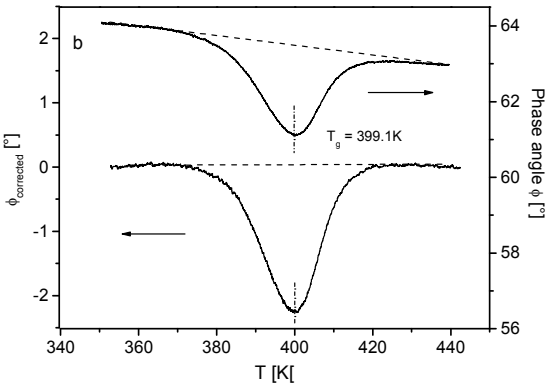

Fig. 3: Real part (a) and phase angle (b) of the complex differential voltage of a thin P2VP polymer film (347 nm) measured at a frequency of 160 Hz. The contribution of the underlying step in the heat capacity in the raw data of the phase angle (upper panel) was subtracted from the all over curve (lower panel).

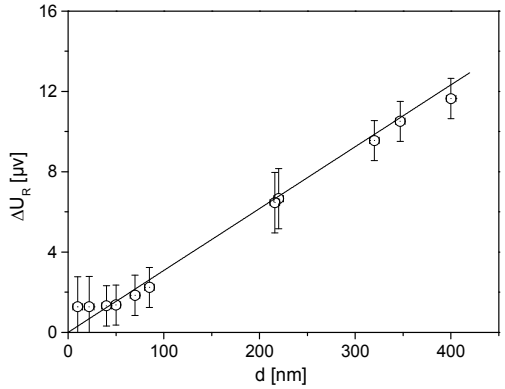

Fig.4: ΔU_R versus the film thickness d for a frequency of 160 Hz. The solid line is a linear regression to the data. For low film thickness the error is somewhat larger. Therefore the data points for the lowest film thickness might deviate slightly from the regression line.

A dynamic glass transition temperature can be determined as either the half step temperature of U_R or as the maximum temperature of the peak of the corrected phase angle. In the raw data of the phase angle (Fig. 3b, upper panel), there is an underlying step in the signal, which is proportional to the real part. Hence, the phase angle is corrected by subtracting this contribution. According to Eq. (1) and assuming that the density of the film is the same as in the bulk, the step high of the heat capacity at the glass transition is given by [40]

$$C_{S,Liquid} - C_{S,Glass} = \frac{i\omega \bar{C}^2 \left(U_{R,Liquid} - U_{R,Glass}\right)}{SP_0} \sim m \sim d \qquad (2)$$

where m is the mass of the film. Therefore, $U_{R,Liquid}$ - $U_{R,Glass}$ = ΔU_R should be proportional to the thickness of the film. In Figure 4, ΔU_R is plotted versus d. The expected linear dependence is confirmed. Moreover, the data can be described by a regression line going through the point of origin. From those results, one might conclude that the whole sample material on the chip takes part in the dynamic glass transition and no boundary layer with a reduced mobility is present.

3.1. Conventional analysis of specific heat spectroscopy data

Figure 5 gives the normalized phase angle versus temperature for different film thicknesses for a frequency of 160 Hz. For all values of d the data collapse into a common curve. This means that the dynamic glass transition temperature is independent of the film thickness. Similar results were obtained by AC-chip calorimetry for PS [19,39], PMMA [50,58], poly(2,6-dimethyl-1,5-phenylene oxide) [40], polycarbonate [41] and also poly(vinyl methyl ether) [42]. At the first glance the results obtained here are in accordance with the dielectric data given in references [20,50] but disagree with findings discussed in [38,48].

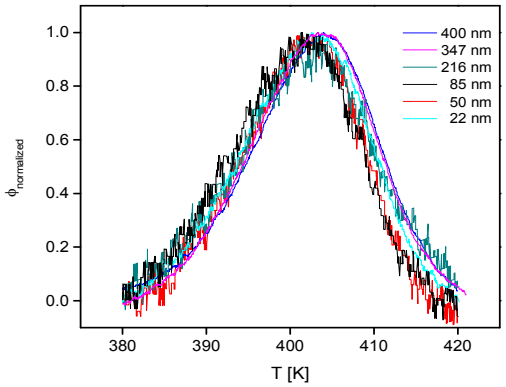

Fig. 5: Normalized phase angle of the complex differential voltage versus temperature measured for thin P2VP films at a frequency of 160 Hz for selected thicknesses of 400, 347, 216, 85, 50, and 22 nm.

To analyse the data in more detail, Gaussians were fitted to the normalized phase angle as depicted in inset A of Fig. 6 [40]. From such analysis, the maximum temperature of the normalized phase angle is estimated at the given frequency and the relaxation map can be constructed (see Figure 6). Within the experimental error of ±3 K, the data for all film thicknesses collapse into one chart. As mentioned above, this is in agreement with AC-chip calorimetry studies on other polymers [19,39-42,58].

The temperature dependence of the relaxation rates can be described by the Vogel/Fulcher/Tammann- (VFT-) equation [59-61]

$$log\ f_p = \log f_\infty - \frac{A}{T - T_0} \qquad (3)$$

where f_∞ and A are fitting parameters and T_0 is called ideal glass transition or Vogel temperature, which is found to be 30-70 K below the thermal T_g. For all film thicknesses the data can be described by a common VFT-fit (see Figure 6). Due to the limited frequency range of the specific heat spectroscopy, the prefactor f_∞

Soft Matter Accepted Manuscript

This journal is © The Royal Society of Chemistry [year]

was taken from the dielectric results (see below) and kept constant during the fit procedure.

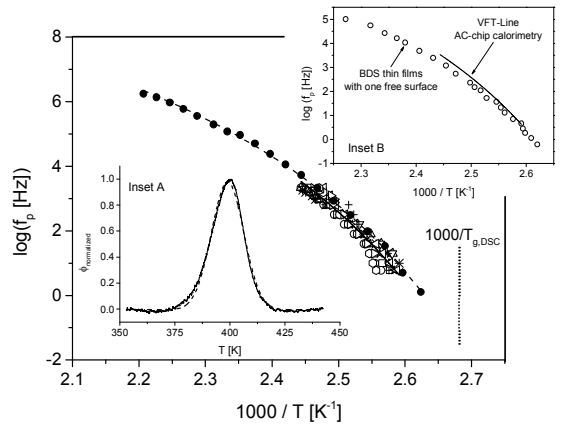

Fig. 6: Relaxation rates versus inverse temperature for different film thicknesses estimated from the normalized phase angle (open symbols): circles – 405 nm, squares – 349 nm, up sited triangles – 230 nm, down sited triangles -216 nm, stars – 150 nm, asterisks – 120 nm, left sited triangles – 85 nm, hexagons – 50 nm, right sited triangles – 22 nm, crosses – 10 nm. The solid circles are data from dielectric spectroscopy for a bulk sample. Solid lines are fits of the VFT equation to the corresponding data with following parameters. Dielectric data (dashed line): log (f_∞ [Hz])=12, A=779 K, T_0=315.4 K; Thermal data (solid line): log (f_∞ [Hz])=12, A=774.6 K, T_0=317.8 K. The dotted line gives the thermal glass transition temperature measured by DSC. Inset A gives the normalized phase angle for a film with a thickness of 347 nm at a frequency of 160 Hz (solid line). The dashed line is a fit of a Gaussian to the data. The solid line is the averaged value of the given data points. Inset B compares dielectric data for ultrathin P2VP films measured with one free surface taken from reference [50] with the VFT-fit taken from the AC-chip calorimetry. The dielectric data are averaged data in the thickness range from 172 nm down to 8 nm because the data for all film thicknesses collapse into one chart.

In Figure 6, the data for a bulk sample measured by dielectric spectroscopy are included as well. Further, the temperature dependence of these data can be described by the VFT equation where the estimated value for the Vogel temperature T_0 is close to that estimated from the thermal data (see caption Figure 6). The dielectric and thermal data overlap more or less, which is a bit uncommon for most materials. The thermal and dielectric data usually exhibits a systematic shift, as previously found for different homopolymers [41,42], and also for low molecular compounds [62].

The inset B of Figure 6 compares dielectric data measured for thin films of P2VP with the VFT fit line extracted from the specific heat spectroscopy data. The dielectric data are the averaged data in the thickness range of 172 nm down to 8 nm, taken form reference [50]. The free surface was implemented by the use of insulating colloids as spacers. For more details see reference [50]. Both sets of data, where samples have one free surface, agree nicely with each other and both sets of relaxation have the same temperature dependence. A similar behaviour should be expected for mechanical measurements, which are hard to conduct in the case of ultrathin films.

3.2. Contact angle measurements

To characterize the interaction of the P2VP segments with the SiO_2 surface of the substrate contact angle measurements were carried out. It is assumed that a silicon wafer with 500 nm native SiO_2 layer has the same surface properties than the used AC-chip. The estimated contact angles obtained for the different test liquids are summarized in Table 1.

Table 1: Contact angle values of the test liquids for poly(2-vinyl pyridine). Data for SiO_2 were taken from reference [41]. The errors result from the average of measurements on 6 drops.

	Water	Formamide	Ethylene glycol	Diiodomethane
P2VP	67.5° ± 0.9°	65.5° ± 0.8°	46.6° ± 1.1°	40.0° ± 0.9°
SiO2	61.0° ± 1.0°	48.2° ± 1.0°	39.0° ± 0.6°	28.9° ± 1.2°

The total surface energy γ^{Total} of a sample is expressed by $\gamma^{Total} = \gamma^{LW}+\gamma^{P}$ where γ^{LW} and γ^{P} are the dispersive and polar components of the surface energy, respectively [63,64]. The measured contact angles θ_i for the liquid i are related by the Owens/Wendt theory [65,66], which is a combination of Young's relation with Good's equation (for details see [67]) to the polar and dispersive components of the surface energies of the solid and liquid by

$$\frac{(1+\cos\theta_i)\gamma_{L,i}}{2\sqrt{\gamma_{L,i}^{LW}}} = \sqrt{\gamma_S^P}\,\frac{\sqrt{\gamma_{L,i}^{p}}}{\sqrt{\gamma_{L,i}^{LW}}} + \sqrt{\gamma_S^{LW}} \qquad (4)$$

where γ_S^P and γ_S^{LW} are the dispersive and polar components of the surface energy of the polymer or the substrate (S=P2VP, SiO_2). The values for the surface tension of the test liquids were taken from reference [63]. Using at least 3 test liquids, an Owens/Wendt plot according to Equ. (4) is created and the polar and dispersive components of the solid surface energy are estimated by linear regression. Results are presented in Table 2.

Table 2: Total surface energy γ^{Total} and its dispersive γ^{LW} and polar γ^{P} components for P2VP and the SiO_2 surface of the silicon wafer.

	γ^{Total} [mJ m^{-2}]	γ^{LW} [mJ m^{-2}]	γ^{P} [mJ m^{-2}]
P2VP	39.5	29.8	9.7
SiO_2	47.0	44.6	2.3

The rule of Fowkes [64] was applied to estimate the interfacial energy γ_{SP} between P2VP and SiO_2, which reads

$$\gamma_{SP} = (\gamma_A + \gamma_{B)} - 2\left[\left(\gamma_A^{LW}\gamma_B^{LW}\right)^{\frac{1}{2}} + \left(\gamma_A^{p}\gamma_B^{p}\right)^{1/2}\right] \qquad (5)$$

where A and B refer to the substrate and the polymer, respectively.

Using Eq. (5) the total interfacial energy between P2VP and SiO_2 is 4.1 mJ m^{-2}. According to reference [35] this is a strong interaction between the polymer segments and the surface of the substrate. Therefore an adsorbed layer with a reduced mobility should be formed at the surface of the substrate in agreement with

Soft Matter Accepted Manuscript

results published in reference [48]. Likewise for other polymers, which interact strongly with the substrate, an increase of the glass transition temperature should be observed. But however, no change in dynamic T_g was observed here by specific heat spectroscopy. One possible reason for this result might be the high molecular weight of the used P2VP. As it was shown in reference [31,71] the formation of the reduced mobility layer depends on time and the diffusive mobility of the polymer chains. For a high molecular weight the chain mobility is lower than for a lower one. It might be that under the selected experimental condition the annealing time above T_g was not long enough to form a reduced mobility at the substrate, which is thick enough to influence the dynamic glass transition of the whole film.

Attempts to correlate the change in the glass transition temperature with the interaction energy between the substrate and the polymer surface γ_{SP} are made in reference [35]. In Figure 7, the difference of the glass transition temperature for 20 nm thick films and the bulk value versus the interfacial energy are plotted for polystyrene and poly(methyl methacrylate) spin coated on modified octadecyltrichlorosilane (OTS) surfaces according to reference [35]. For γ_{SP}<2 mJ m^{-2} a depression of the glass transition temperatures should be observed while for γ_{SP}>2 mJ m^{-2} an increase of T_g should be observed. In this figure, data for different polymer substrate combinations, with comparable film thicknesses, taken from the literature, were added. (A similar figure but with less data points is given in reference [68] too). This concept is able to describe the variation of the T_g with interaction energy for polystyrene and poly(methyl methacrylate) on the modified octadecyltrichlorosilane surfaces. Also for some other polymers like polycarbonate on SiO_2 or AlO_X [32,41] or poly(ethylene terephthalate) [69], this correlation seems (partially) valid. However, it is not generically true for all polymer/substrate combinations.

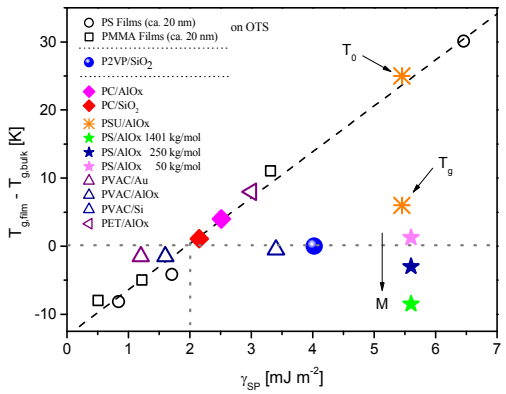

Fig.7: Difference of the glass transition temperature for 20-nm-thick films and the corresponding bulk value versus the interfacial energy. The open symbols for poly(methyl methacrylate) (squares) and polystyrene (circles) are taken together with the (dashed) correlation line from reference [35]. The grey dotted lines gives ΔT_g=0 and critical value for γ_c. The data for polycarbonate (PC,diamonds) are taken from reference [32] (AlOx) and [41] (SiO_2). The asterisks represent data for polysulfone (PSU) taken from reference [33]. The value for PET (left pointed triangle) are taken form reference [69]. The data for poly(vinyl acetate) (PVAC, triangels) prepared on the indicated surfaces are taken from reference [70]. The values for polystyrene (PS, green stars) are drawn from [71]. P2VP (solid circle) – this work.

For instance, for polysulfone, the interaction energy between the segments and the substrate surface was estimated to be γ_{SP}= 5.45 mJ m^{-2}, taken from reference [33]. This value is much larger than the value of polycarbonate/AlO_X, where a similar increase of the glass transition temperature of about 5 K (for a ca. 20 nm thick film) was found. However, the corresponding point for polysulfone is located far away from the correlation line between the polymer-substrate interaction energy and the change in the glass transition temperature. However, by taking the Vogel temperature, T_0, as a measure for the thermal glass transition temperature, the correlation between the change in the glass transition temperature and the polymer-substrate interaction energy [31,35] seems to be fulfilled.

For poly(vinyl acetate) films prepared on different surfaces [70], this correlation is found to be invalid as well. Data for polystyrene samples having different molecular weights were also added [71]; whereas the interaction energy between the AlO_X surface of the substrate and the polystyrene segments is taken from reference [31]. These data points are located also far away from the correlation line between the polymer / substrate interaction energy and the change in the glass transition temperature. The observed dependence on the molecular weight is in contradiction to the assumption that the interaction energy between the polymer segments and the surface of the substrate is the only parameter, which determines the value of the glass transition temperature of ultrathin polystyrene films as well. This regards also the observed time dependence of the depression of T_g [31]. In conclusion, the polymer/substrate interaction energy seems to be not the only parameter, which is responsible for the change in the thermal glass transition temperature with the film thickness for ultrathin films. Packing effects and/or densifications of the reduced mobility layer at the surface, which can be time and molecular weight dependent, might also play a role. This is discussed also in detail in reference [31].

3.3. Derivative analysis of specific heat spectroscopy data

As discussed above, all AC-chip calorimetry studies on ultrathin films of homopolymers, including P2VP used in this work concluded that the dynamic T_g is thickness independent, in many cases, contradicting the findings of other studies using different characterization techniques. For P2VP, one shall expect to see a rather strong reduced mobile layer as speculated from the contact angle measurements, shown above. The reduced mobile layer for this polymer has also been detected by other methods, e.g. X-ray reflectivity [38] and different BDS studies [46,48]. On the other hand, also the existence of a high mobile free surface layer has been evidenced for P2VP [52]. To resolve the systematic contradiction of AC-chip calorimetry from the other characterization method, an advanced analysis of the calorimetric data might be useful.

From the technical point of view, there are a few problems with the conventional data analysis of AC-chip calorimetry. Firstly, the theoretical treatment of the method assumes that the reference and the sample sensor are identical. In that theoretical case, one shall expect to see a constant baseline at zero level for the differential voltage for all frequencies and temperatures. Because of the fact that the sensors are not completely identical, an extra contribution will be added up to the signal coming from the film. This extra contribution to the differential voltage is not large but depends on both temperature and frequency. It can be ignored for relatively thick films (>50 nm). However, for thinner films, the difference between the two empty sensors is in the same order of magnitude as the measured U_R, which might induce artifacts.

Soft Matter Accepted Manuscript

This journal is © The Royal Society of Chemistry [year]

The other problem in estimating the dynamic glass transition temperature from the maximum position of the phase angle is related to the fact that the measured phase angle has also an underlying contribution that is proportional to the step of the heat capacity [39]. This effect will not affect the T_g peak position for thick samples. However, for ultrathin films (<20 nm), the values of the phase angle become small and comparable to the noise level of the instrument [40]. Thus, the correction and estimation of the phase angle cannot be done unambiguously.

For these reasons here the temperature dependence of the complex differential voltage is analysed in more detail for some selected sample thicknesses, which was investigated with an optimized sensitivity. First, the sensitivity of the lock-in amplifier of the AC-chip calorimeter was set to be between two and three times the value of U_R of the sample at 160 Hz and the corresponding $T_{g,160\ Hz}$, to assure an optimal signal and a reduced noise. Second, pairs of empty sensors were first measured in the identical frequency and temperature range as for the samples to obtain the excess contribution of the sensors. Third, after the measurement of the films spin coated on one of the analyzed empty sensors, the real part of the complex voltage obtained for the two empty sensors was subtracted from the corresponding U_R recorded for the films. This procedure leads to a corrected U_R.

Instead of analysing the temperature dependence of the phase angle, the derivative of the corrected real part of the complex voltage versus temperature was employed. Since U_R changes step-like at the dynamic glass transition, its first derivative will result in a peak. The temperature of the peak maximum can be taken as the dynamic glass transition temperature at 160 Hz. The derivative method will also allow estimating dU_R/dT which is related to dc_p/dT for both the glassy and the liquid state. To calculate the derivative of the corrected real part of the complex voltage was adjacent-point averaged (over 300 points; for the two thinnest films over 500 points) in the whole measured temperature range. This will result in a smoothed signal. To have equidistant points, U_R (T) was interpolated (1000 points). After that the derivative was calculated. It is worth to mention that the difference in the smoothing methods and parameters was previously reported to result in about ±2 K difference in the T_g values, which is within the uncertainty of the measurement [40]. The advantage of this method is strong when analyzing measurements of ultrathin films, where the signal is weak and changes of the phase angle are hardly to detect. For films thinner than 15 nm, one can usually still see a small step in U_R, yet it is not unambiguously to determine where the step starts and ends. Moreover, in a first crude approximation the derivative can be considered as a representation of the relaxation time spectra [72].

Four new samples were prepared (10 nm, 20 nm, 85 nm and 220 nm) and the measurements were analyzed as described above.

Figure 8 shows the derivative calculated as described versus temperature for three different sample thicknesses at a frequency of 160 Hz. For each value of the thicknesses a well-defined peak is visible indicating the dynamic glass transition. With decreasing thickness a systematic shift of the dynamic glass transition to lower temperatures is observed. This shift up to 7 K is essentially larger than the error of the AC-chip calorimetric measurement.

The derivative method was also applied to the other samples prepared previously and a dynamic glass transition temperature at 160 Hz was estimated from the maximum position of the derivative. These data were plotted in Figure 9 versus the thickness of the film. The dynamic glass transition temperature of the bulk sample is taken as the average value of the dynamic glass transition temperature for the five samples with the highest thicknesses.

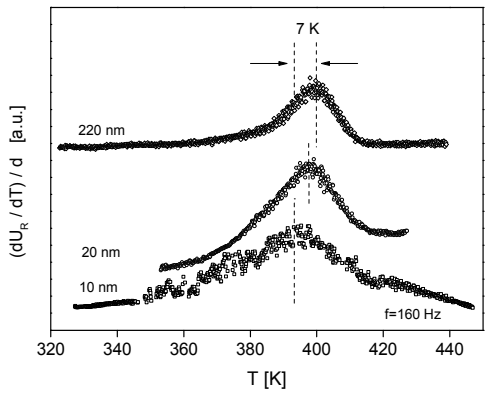

Fig. 8: Derivative of the corrected real part of the complex differential voltage with regard to temperature versus temperature for the indicated film thicknesses at the frequency of 160 Hz. For sake of clearness the curves were shifted along the y-scale.

For small film thicknesses, the value of the dynamic glass transition is below this average value and further decreases with decreasing film thickness. Because a decrease of the dynamic glass temperature is considered as the influence of a free surface [11], this result can be considered as an evidence for a free surface with a higher molecular mobility from calorimetric measurements.

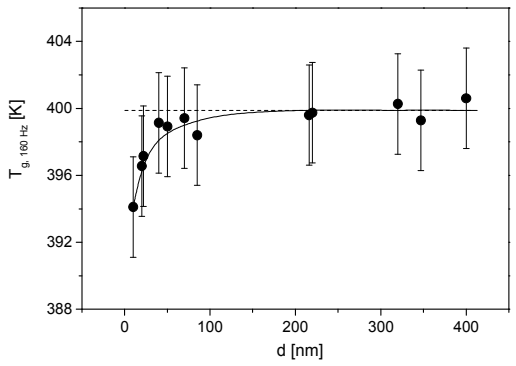

Fig. 10**:** Dynamic glass transition temperature measured at 160 Hz versus film thickness d. The dashed line is the average value of the five data points with largest thicknesses.

It should be shortly summarized why the traditional and the derivative based data analysis give different results. Firstly, in the phase angle two different quantities with well-defined physical meanings are mixed up, the real and the loss part of the complex differential voltage. The correction of the phase angle for the real part of the complex voltage cannot be done unambiguously especially for low film thickness as discussed above. Secondly, the derivative of the real part of the complex differential voltage can be considered as an estimation of the underlying relaxation time spectra [72]. This means both quantities weight the underlying dynamics in a different way. This fact in unimportant for thick films but might become relevant for low film thicknesses. A closer inspection of Figure 5 that also the phase

Soft Matter Accepted Manuscript

angle measured for higher thickness seem to be located at somewhat higher temperatures which is consistent with the derivative analysis.

Some further evidence for a mobile surface layer comes from the shape of dU_R/dT versus temperature. A more detailed inspection of Figure 8 reveals that the width of the derivative for a thin film (for instance see 10 nm) is broader than that measured for a larger thickness. This fact is illustrated in more detail in Figure 11, where the derivative for a 10 nm and a 40 nm thick film are compared. Therefore, the derivative is normalized with respect to both its intensity and peak temperature. Figure 11 reveals that the peak for the 10 nm thick film is much broader than that for the 40 nm one. Firstly, compared to the 40 nm thick layer, the film with a thickness of 10 nm shows a considerable broadening at the lower temperature side. In the sense of distribution of relaxation times, this corresponds to an increased contribution of relaxation modes having shorter relaxation times. With decreasing film thickness, the influence of a surface layer with a higher mobility will increase. Therefore, in addition to the decrease of the dynamic glass transition with decreasing film thickness, the broadening of the relaxation spectra on the low temperature side gives further evidence for the existence of a surface layer with a higher molecular mobility at the polymer air interface.

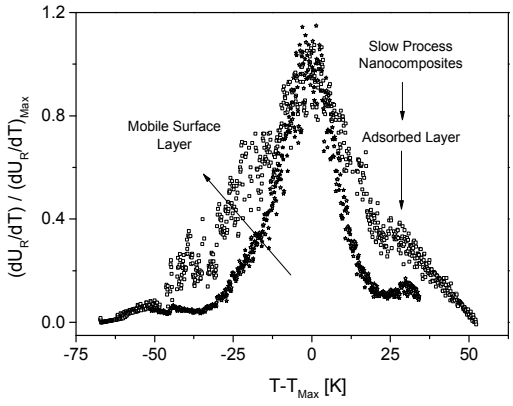

Fig. 11: Normalized derivative $(dU_R / dT) / (dU_R / dT)_{Max}$ versus temperature at a frequency of 160 Hz for a 10 nm (open squares) and a 40 nm (open stars) thick film.

Besides the broadening of the spectra at the low temperature side for the thin film for the 10 nm thin film there is also a broadening of the derivative at temperatures above the dynamic glass transition temperature. This broadening at the high temperature side of the spectra is due to relaxation modes having a reduced mobility. As shown by the contact angle measurements, discussed above, the P2VP segments should strongly interact with the SiO_2 surface of the sensor, which should result in slowing down of the molecular dynamics of the polymer segments close to the surface. Therefore, the broadening of the spectra at high temperatures is assigned to polymer segments, which are in interaction with the SiO_2 surface of the sensor. A corresponding broadening was observed by dielectric spectroscopy employing nanostructured electrodes [20]. A closer inspection of the data for the 10 nm thick film reveals that there is a small shoulder at $T-T_{Max}$=28 K (T=424 K). This shoulder is found at the same temperature frequency position, where for the nanocomposites of P2VP with silica nanoparticles, discussed in reference [48], the relaxation process is observed, which was related to the fluctuations of P2VP segments adsorbed at the surface of the silica particles. This coincidence provides further evidence that a reduced mobility layer is formed at surface of the calorimeter. Probably, due to the high molecular weight of the used P2VP, the formation of this reduced mobility layer will take longer time. Under the employed experimental conditions, it is likely that the thickness of this layer is small and will not influence the dynamic glass transition behavior of the whole film. For future work, additional investigations are planned where the annealing time and temperature, during film preparation, are varied in broader ranges. This includes further a variation of the molecular weight because it was shown for instance that for polystyrene [71] the change of the glass transition temperature depends on molecular weight due to a changed adsorption kinetics.

It is well known that the specific heat capacity in the glassy state has a stronger temperature dependence than in the liquid [73], which means $(dc_p/dT)_{Glass} > (dc_p/dT)_{Liquid}$. Close to the glass transition $c_p(T)$ can be approximated by linear dependencies in both the glassy and liquid state. In the derivative representation, this is reflected by constant values of the derivative dU_R/dT which corresponds to dc_p/dT independent of temperature below and above the dynamic glass transition. The inset of Figure 12 depicts the derivative versus temperature for a relatively thick film of 347 nm. For this film, which can be considered as bulk-like, the expected relationship $(dc_p/dT)_{Glass} > (dc_p/dT)_{Liquid}$ is fulfilled. However, Figure 12 shows further that with decreasing film thickness, this relationship changes. For a film with a 220 nm thickness, $(dU_R/dT)_{Glass} \approx (dU_R/dT)_{Liquid}$ holds; whereas for a thinner film with a thickness of 70 nm the relationship is reversed $(dU_R/dT)_{Glass} < (dU_R/dT)_{Liquid}$. This is not only observed for the considered thicknesses, but also for the other thicknesses as well (see Figures 8 and 11). Obviously, confinement effects influence the temperature dependencies of the specific heat capacity in the liquid and glassy state. Such change in the temperature dependence of specific heat capacity before and after the dynamic glass transition region was able to be observed at relatively high thicknesses, above 220 nm in the present study. The critical thickness is possibly molecular weight dependent, which needs further quantitative measurements. It was already reported that for PS with Mw=1400 kg/mol, a change in the temperature dependence of specific heat capacity at the glass transition occurred from several hundred nm [43]. In the glassy state, $c_p(T)$ originates from vibrations. The same vibrations are also responsible for the temperature dependence of the thermal expansion. The specific heat capacity and the thermal expansion coefficient are linked to each other [74]. It has been reported previously that the thermal expansion coefficient in the glassy state for thin films decreases with the film thickness [75,76].

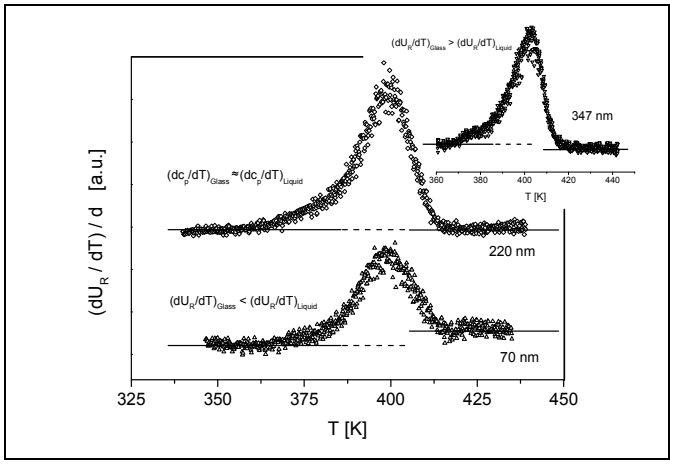

This journal is © The Royal Society of Chemistry [year]

Soft Matter Accepted Manuscript

Fig. 12: Derivative (dU_R / dT) /d versus temperature at a frequency of 160 Hz for a 220 nm (open diamonds) and a 70 nm (open triangles) thick film. The inset shows the same for a film with a thickness of 347 nm.

These findings are quite similar to the results found here for P2VP. Moreover, quasielastic neutron scattering experiments for thin films of polystyrene and polycarbonate [77, 78] showed that the mean square displacement $\langle r^2 \rangle$ decreases with decreasing film thickness. Also a direct investigation of the vibrational density of states in the frequency range of excess vibrations characteristic for the glassy state (Boson Peak) show a decrease of the intensity of the Boson Peak with decreasing film thickness for polystyrene for relatively high thicknesses of 100 nm [79,80]. This behavior is equivalent to a decrease of the mean square displacement. Using a harmonic approximation $\langle r^2 \rangle$ can be related to a force constant f_K by $f_K \sim 1/\langle r^2 \rangle$. A decrease of the mean square displacement can therefore be explained by an increase of the force constant. This means a change from a soft to hard potential. Taking as well as anharmonic contributions into account, the change of the temperature dependence of the specific heat capacity in the glassy state might be explained by a hardening of the potential of the vibrations. However, it is worth to note that the change of the specific heat capacity in the glassy and liquid state might also be explained by a three layer model which also applies here [81]. To differentiate between both possibilities, additional investigations on a broader range of samples and different polymers are required. Such studies are under preparation, which will also including a more quantitative discussion.

4. Conclusion

Specific heat spectroscopy employing differential AC-chip calorimetry in the frequency range from 1 Hz to 10^4 Hz with a sensitivity of pJ/K was used to study the dynamic glass transition behavior of ultrathin poly(2-vinyl pyridine) films with thicknesses from 405 nm down to 10 nm. To characterize the interaction of the P2VP segments with the surface of the substrate, contact angle measurements was utilized along with AFM investigation to study the topology of the films. Broadband dielectric spectroscopy was used to obtain the molecular dynamics for the bulk sample.

AC-chip calorimetry delivers the real part and the phase angle of the complex differential voltage as a measure of the complex heat capacity as function of temperature and frequency simultaneously. The data were analyzed by two different methods. In a rather traditional data analysis, the dynamic glass transition temperature is estimated from the maximum position of the measured phase angle. These data showed no thickness dependence of the dynamic glass transition temperature down to ca. 22 nm, within in the error of the measurement of ± 3 K. This result is in agreement with dielectric data obtained for samples having one free surface, yet still in disagreement to other literature data. Therefore second method was established which is based on the first derivative of the real part of the complex differential voltage with regard to temperature. These data show a decrease of the dynamic glass transition temperature with decreasing thickness of about 7 K. This decrease can be explained as a result of the influence of surface layer with a higher molecular mobility. Moreover, for thin films the data showed a broadening at the lower temperature side of the dynamic glass transition, which can be considered as a further prove for a surface layer.

Moreover, contact angle measurements showed that the P2VP/SiO_2 interaction was rather a strong one, 4.1 mJ m^{-2}, which suggests that an absorbed layer of reduced mobility should exist at the polymer/substrate interface. An absorbed layer was evidenced for films below 50 nm, through another broadening of the peak with the appearance of a shoulder at the higher temperature side of the spectra that superimposes with the fluctuations of P2VP segments adsorbed at the surface of the silica particles, as reported in literature.

Finally, evidence was provided the temperature dependence of the specific heat capacity in the glassy and the liquid state changes depends on the film thickness. These changes were observed for relatively high film thickness of some 100 nm and can be considered as confinement effects. For the glassy state these changes are in agreement with several neutron scattering studies and can be explained by a hardening of the potential of the vibrations, and thus the existence of a reduced mobile layer, in agreement of the three layer model. Nevertheless additional investigations are required.

Acknowledgements

The authors gratefully acknowledge the financial support from the German Science Foundation (Deutsche Forschungs-gemeinschaft, SCHO-470/20-1 and SCHO-470/20-2) is highly acknowledged.

Notes and references

[a]. *BAM Federal Institute for Materials Research and Testing, Unter den Eichen 87, D-12200 Berlin (Germany). Fax: +49 30 / 8104-1617; Tel: +49 30 / 8104-3384;email:andreas.Schoenhals@bam.de*

[b]. *Stranski-Laboratorium für Physikalische und Theoretische Chemie/ Institut für Chemie, Technische Universität Berlin, Straße des 17. Juni 124, 10623 Berlin (Germany)*

1 B.D. Hall, P. Underhill and J.M. Torkelson, *Polymer Eng. Sci*. **1998**, 38, 2039-2045.
2 P.G. Debenedetti and F.H. Stillinger, *Nature,* **2001**, 410, 259–267.
3 P.W. Anderson, *Science,* **1995**, 267, 1617.
4 Ediger, M.; Horrowell, P. *Journal of Chemical Physics* **2012**, 137, 080901-080915.
5 C.A. Angel, *Science,* **1995**, 267, 1924-1935.
6 S. Sastry, P.G. Debendetti and F.H. Stillinger, *Nature,* **1998**, 393, 554-557.
7 H. Yin, S. Madkour and A. Schönhals, Glass transition of ultra-thin polymer films: A combination of relaxation spectroscopy with surface analytics in *Dynamics in confinement: Progress in Dielectrics,* Kremer, F. (Ed.) *Springer*, Berlin **2014**, pp17-59
8 M. Alcoutlabi and G.B. McKenna, *J. Phys. Condens. Matter,* **2005**, 17, 461–524.
9 J.L. Keddie, R.A.L Jones and R.A. Cory, *Faraday Discussions,* **1994**, 98, 219-230.
10 J.L. Keddie, R.A.L Jones and R.A. Cory, *Euro. Phys. Lett.* **1994**, 27, 59-64.
11 M. Ediger and J. Forrest, *Macromolecules,* **2014**, 47, 471-478.
12 J. Forrest and K. Dalnoki-Veress, *ACS Macro Letters* **2014**, 3, 310−314
13 P.A. O'Connell and G.B. McKenna, *Science,* **2005**, 307, 1760–1763.
14 K. Paeng, S.F. Swallen and M. Ediger, *J. Am. Chem. Soc.* **2011**, 133, 8444–8447.
15 J. Forrest and K. Dalnoki-Veress, *J. Coll. Int. Sci*. **2001**, 94, 167–195.

Soft Matter Accepted Manuscript

16 J. Forrest, *Eur. Phys. J. E.* **2002**, 8, 261–266.
17 Z. Fakhraai, J. Forrest, *Science,* **2008**, 319, *600-604*.
18 Y. Chai, T. Salez, J.D. McGraw, M. Benzaquen, K. Dalnoki-Veress, E. Raphaël and J. Forrest. *Science,* **2014**, 343, 994-999.
19 M. Tress, M. Erber, E.U. Mapesa, H. Huth, J. Müller, A. Serghei, C. Schick, K.-J Eichhorn, B. Voit and F. Kremer, *Macromolecules,* **2010**, 43, 9937−9944.
20 M. Tress, E.U. Mapesa, W. Kossack, W.K. Kipnusu, M. Reiche and F. Kremer, *Science,* **2013**, 341, 1371−1374.
21 K. Dalnoki-Veress, J. Forrest, C. Murray, C. Gigault and J.R. Dutcher, *Phys. Rev. E.* **2001**, 63, 031801-031811.
22 S. Napolitano, A. Pilleri, P. Rolla and M. Wübbenhorst, *ACS Nano,* **2010**, 4, 841-848.
23 E.C. Glor and Z. Fakhraai, *J. Chem. Phys.* **2014**, 141, 194505.
24 V. Lupaşcu, S.J. Picken and M. Wübbenhorst, *Journal of Non-Crystalline Solids,* **2006**, 352, 5594-5600.
25 Z. Fakhraai and J.A. Forrest, *Phys. Rev. Lett.* **2005**, 95, 025701-025705.
26 N. Shamim, Y.P. Koh, S. L. Somon and G. B. McKenna, *J. Polym. Sci. Part B: Polym. Phys*. *2014*, 52, 1462-1468.
27 J.S. Sharp and J.A. Forrest, *Phys. Rev. Lett.* **2003**, 91, 235701-235705.
28 K. Paeng, R. Richert and M.D. Eidger, *Softmatter,* **2012**, 8, 819-826.
29 D. Qi, M. Ilton and J.A. Forrest, *Eur. Phys. J. E,* **2011**, 34, 56-63.
30 D. Qi; C.R. Daley, Y. Chai and J.A. Forrest. *Soft Matter,* **2013**, 9, 8958−8964.
31 S. Napolitano and M. Wübbenhorst, *Nature Communications,* **2011**, 2, 260-267.
32 H. Yin, S. Napolitano and A. Schönhals, *Macromolecules,* **2012**, 45, 1652-1662.
33 D. Labahn, R. Mix and A. Schönhals, *Physical Review E,* **2009**, 79, 011801-011810.
34 C. Rotella, M. Wübbenhorst and S. Napolitano, *Soft Matter,* **2011**, 7,5260-5266.
35 D.S. Fryer, R.D. Peters, E.J. Kim, J.E. Tomaszewski, J.J. de Pablo, P.F. Nealey, *Macromolecules,* **2001**, 34, 5627-5634.
36 A. Clough, D. Peng, Z. Yang, and K. O. Tsui, K. *Macromolecules,* **2011**, 44, 1649–1653.
37 C.J. Ellison and J.M.Torkelson, *Nat Mater.* **2003**, 2, 695-700.
38 J.H. van Zanten, W.E. Wallace and W. Wu, *Physical Review E,* **1996**, 53, R2053-R2056.
39 H. Huth, A. Minakov and C. Schick, *J. Polym. Sci. B: Polym. Phys*. **2006**, 44, 2996-3005.
40 D.S. Zhou, H. Huth, Y. Gao, G. Xue and C. Schick, *Macromolecules,* **2008**, 41,7662-7666.
41 H. Yin and A. Schönhals, *Soft Matter,* **2012**, 8, 9132-9139.
42 H. Yin and A. Schönhals, *Polymer,* **2013**, 45, 2067-2070.
43 V.M. Boucher, D. Cangialosi, H. Yin, A. Schönhals, A. Alegria and J. Colmenero, *Soft Matter,* **2012**, 8, 5119-5122.
44 C.H. Park, J.H. Kim, M. Ree, B.H. Sohn, J.C. Jung and W.C. Zin, *Polymer*, **2004**, 45, 4507–4513.
45 C.B. Roth, K.L. McNerny, W.F. Jager and J.M. Torkelson, *Macromolecules,* **2007**, 40, 2568–2574.
46 S. Napollitano,V. Lupaşcu and M. Wübbenhorst, *Macromolecules,* **2008**, 41, 1061-1063.
47 J. Moll and S.K. Kumar, *Macromolecules*, **2012**, 43, 1131-1135.
48 A. Holt, P. Griffin, V. Bocharova, A. Agapov, A. Imel, M. Dadmun, J. Sangoro and A. Sokolov, *Macromolecules,* **2014**, 47, 1837–1843.
49 M. Füllbrandt, P. Purohit and A. Schönhals, *Macromolecules,* **2013**, 46, 4626-4632.
50 A. Serghei, H. Huth, C. Schick and F. Kremer, *Macromolecules,* **2008**, 41, 3636-3639.
51 M. Efremov, E. Olson, M. Zhang, Z. Zhang and L. Allen, *Phys. Rev. Lett*. **2003**, 91, 085703-085707
52 K. Paeng, R. Richert and M.D. Ediger, *Soft Matter,* **2012**, 8, 819-826.
53 S. van Herwaaden, *Application note for Xsensor's calorimtere chips of XEN-39390 series* http://www.xensor.nl/pdffiles/sheets/nanogas3939.pdf
54 C. Schick *Calorimetry in Polymer science: A comprehensive reference*, Matyjaszewwski, K. Möller (Eds) Elsevier B. V., Amsterdam, **2012**, pp 793-823
55 H. Huth and C. Schick, *Personal Communication*.
56 G. Reiter, M. Hamieh, P. Damman, S. Sclavons, S. Gabriele, T. Vilmin and E. Raphael, *Nat. Mater.* **2005**, 4, 754-758.
57 H. Huth and C. Schick, *Personal Communication*.
58 H. Huth, A. Minakov, A. Serghei, F. Kremer and C. Schick, *Eur Phys J-Spec Top,* **2007**,141,153-60.
59 H. Vogel, *Phys. Z.* **1921**, 22, 645.
60 G. Tammann and G. Fulcher, *J. Am. Ceram. Soc.* **1925**, 8, 339.
61 W. Hesse, *Anorg. Allg. Chem*. **1926**, 156, 245.
62 B. Jacobson, T. Hecksher, T. Christensen, N.B. Olsen, J.C. Dyre and K. Niss, *J. Chem Phys*. **2012**, 136, 081102-081107.
63 L. Lee, *Langmuir,* **1996**, 12,1681-1687.
64 R. Good and L. Girifalco, *J. Phys. Chem*. **1960**, 64, 561-565.
65 D. Owens and R. Wendt, *J. Appl. Polym. Sci.* **1969**, 13, 1741-1747.
66 D.J. Kaelble, *Adhesion,* **1970**, 2, 66-81.
67 C. van Oss, M. Chaudhury and R. Good, *Chem. Rev*. **1988,** 88, 927-931.
68 S. Napolitano, S. Cappoini, B. Vanroy, *Eur. Phys. J. E,* **2013**, 36, 61-65.
69 S. Napolitano, D. Prevosto, M. Lucchesi, P. Pinque, M. D´Acunto and P. Rolla, *Langmiur,* **2007**, 23, 2103-2109.
70 H. Nguyen, M. Labardi, S. Capaccioli, M. Lucchesi, P. Rolla and D. Prevosto, *Macromolecules,* **2012**, 45, 2138-2144.
71 H. Yin, D. Cangialosi and A. Schönhals, *Thermochimica Acta,* **2013**, 566, 186-192.
72 J. van Turnhaut and M. Wübbenhorst, *J. Non-Cryst. Solids,* **2002**, 305, 40-49.
73 Materials.springer.com
74 L.D. Landau and EM. Lifschitz, *Textbook of theoretical physics, vol. V. Statistical physics*, **1979**, Akademie Verlag, Berlin.
75 D.J. Pochan, E.K. Lin, S.K. Satija and W.Wu, *Macromolecules,* **2001**, 34, 3041-3045.
76 T. Miyazaki, K. Nishida and T. Kanaya, *Phys. Rev. E,* **2004**, 69, 061803.
77 R. Inoue, T. Kanaya, H. Yamano, K. Nishida, I. Tsukushi and K. Shibata, *AIP Conf. Proc.* **2003**, 708, 197.
78 C.L. Soles, J.F. Douglas, W. Wu and R.M. Dimeo, *Phys. Rev. Lett.* **2002**, 88, 037401.
79 R. Inoue, T. Kanaya, H. Yamano, K. Nishida, I. Tsukushi and K. Shibata, *Phys. Rev. Lett.* **2005**, 95, 056102.
80 R. Inoue, T. Kanaya, H. Yamano, K. Nishida, I. Tsukushi and K. Shibata, *Phys. Rev. E,* **2006**, 74, 021801.
81 M. Bhattacharya, M.K. Sanyal, T.H. Geue and U. Pietsch, *Phys. Rev. E,* **2005**, 71, 041801.

Soft Matter Accepted Manuscript

This journal is © The Royal Society of Chemistry [year]

For Table of Contents use only

Calorimetric evidence for a mobile surface layer in ultrathin polymeric films: Poly(2-vinyl pyridine)

Sherif Madkour, Huajie Yin, Marieke Füllbrandt, Andreas Schönhals

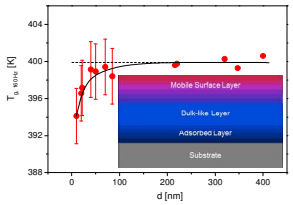

Soft Matter Accepted Manuscript